ICIC Express Letters
Part B: Applications
Volume **14**, Number **5**, May **2023**

ICIC International ©2023 ISSN 2185-2766
pp. **491–498**

DEVELOPMENT OF STEP-UP/STEP-DOWN SINGLE INDUCTOR AC/DC CONVERTERS FOR ENERGY HARVESTING SYSTEMS

Yoshiki Kino*, Daigo Nakashima and Kei Eguchi

Graduate School of Engineering
Fukuoka Institute of Technology
3-30-1, Higashi-Wajiro, Higashi-ku, Fukuoka-shi, Fukuoka 811-0295, Japan
mam21105@bene.fit.ac.jp; eguti@fit.ac.jp
*Corresponding author: mam22107@bene.fit.ac.jp

Received October 2022; accepted January 2023

Abstract. *In recent years, energy harvesting technology has attracted much attention in the field of power-saving applications. Energy harvesting is a technology that collects unused micro energy around us and converts it into electricity. Among others, vibration energy harvesting requires an AC/DC converter to convert the vibration energy into a stepped-up DC voltage. In this study, we propose three types of AC/DC converters that can realize various voltage gains by changing the duty ratio. Unlike the conventional converters with constant voltage gains, the proposed converters feature a hybrid topology that combines a multiple-input/single-output (MISO) Dickson converter with a traditional boost or buck or buck-boost converter. Simulation results show that 1) the proposed circuit with a boost converter can achieve the 11∼26 times gain, 2) the proposed circuit with a buck converter can realize the 2.4∼6.6 times gain, and 3) the proposed circuit with a buck-boost converter can provide voltage gains from −3.1 to −19.6. Furthermore, experimental results demonstrated that the voltage gain of all proposed circuits can be changed by varying the duty ratio in the range of 0.3∼0.7. From these results, the feasibility of the proposed topology is confirmed experimentally.*
Keywords: Energy harvesting, Dickson converter, Boost converter, Buck converter, Buck-boost converter

1. **Introduction.** In recent years, energy harvesting technology attracts attention in the field of small power applications. As described in [1,2], the energy harvesting technology takes an important role in sensor networks. The energy harvesting system gathers minute energy, such as light energy, electromagnetic wave energy, thermal energy, and vibrational energy, and converts the minute energy into electricity [3]. Specifically, the method that converts pressure [4], electromagnetic waves [5], heat [6], and light [7] into electric power has been proposed. In this paper, we focused on engine vibration as an energy harvesting source.

To convert engine vibration energy into electric power, an AC/DC converter that converts AC signals into DC electric power is required. Various AC/DC converters have been proposed so far. For example, Shi et al. [8] proposed the AC/DC converter which put full wave rectifier and two buck boost converters together. Shareef et al. [9] developed the circuit which does not need a rectifier circuit. However, it is difficult to provide a high voltage gain from constant voltage. Abe et al. [10] designed the AC/DC converter using switched capacitor (SC) techniques. Since this AC/DC converter does not use magnetic component, there is an advantage that electromagnetic interference (EMI) is small. However, it provides a stepped-down voltage only. Eguchi and Shibata [11] realized a multiple-input single-output (MISO) AC/DC converter for the vibration energy harvesting. However, the application of this MISO AC/DC converter is limited, because

DOI: 10.24507/icicelb.14.05.491

the voltage gain is constant. Therefore, the circuit must be reconfigured according to the voltage required which takes time and effort. Do et al. [12,13] designed a new type of switched capacitor converter with cross-connecting Fibonacci topologies [14]. By using the cross-connecting Fibonacci topologies, this converter can achieve high voltage gains. However, it requires many transistor switches.

To derive a DC voltage from unstable vibration energy inputs, we design AC/DC converters with flexible voltage gain control. Specifically, three types of AC/DC converters that can realize various voltage gains are proposed in this paper. Unlike the conventional converters with constant voltage gains, the proposed converters feature a hybrid topology that combines a multiple-input/single-output (MISO) Dickson converter [15] with a traditional non-isolated converter, i.e., boost or buck or buck-boost converter. The proposed MISO AC/DC converter using the boost converter is used for high voltage applications, the proposed MISO AC/DC converter using the buck converter is applied for low voltage applications, and the proposed MISO AC/DC converter using the buck-boost converter is employed for the applications using negative voltages.

The structure of this paper is as follows. At first, Section 1 describes the background of this research, the problems with conventional circuits, and the purpose of this research. Section 2 explains the circuit configuration and operation of the proposed circuits. Section 3 shows the effectiveness of the proposed circuits through the comparison with conventional circuits. Section 4 verifies the validity of the circuit topology of the proposed circuit by conducting experiments. Finally, Section 5 presents the conclusion of this work and describes the future work of this research.

2. **Circuit Configuration.** Figure 1 illustrates the circuit diagram of the conventional circuit [15]. As this figure shows, the conventional circuit connects two Dickson converters with four stages in series. If the voltages of two input sources are the same, the output voltage of each Dickson converter with four stage is given by

$$V_{o1} = 4(V_{in} - V_{th}) \tag{1}$$

where V_{o1} represents the output voltage of the four-stage cascaded Dickson converter, V_{in} denotes the input voltage, and V_{th} is the diode threshold voltage. Since the conventional circuit consists of two Dickson converters, the output voltage is expressed as

$$V_{out} = 4(V_{in} - V_{th}) + 4(V_{in} - V_{th}) = 8(V_{in} - V_{th}) \tag{2}$$

In Equation (2), V_{out} represents the output voltage.

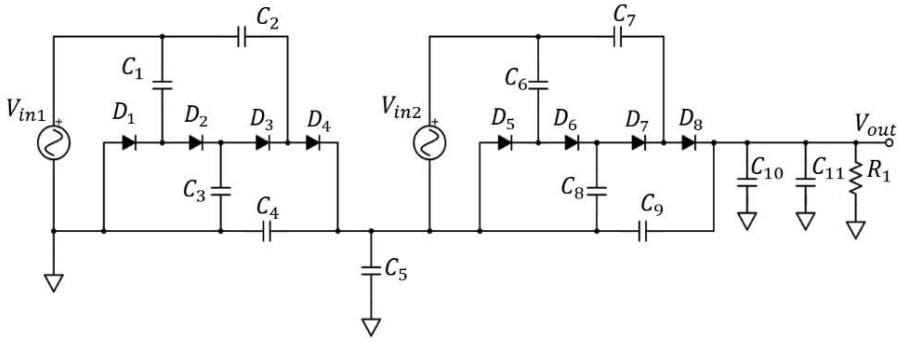

FIGURE 1. Circuit diagram of the conventional circuit

Figure 2 shows the instantaneous equivalent circuits of the Dickson converter. The voltage is boosted by repeating two states: state 1 and state 2. Figure 2(a) shows the instantaneous equivalent circuit when the input voltage V_{in} is negative. During state 1, the diodes D_1 and D_3 are driven by the negative input voltage. As a result, the capacitors C_1 and C_2 are charged. Next, the input voltage V_{in} switches positively. Figure 2(b) shows

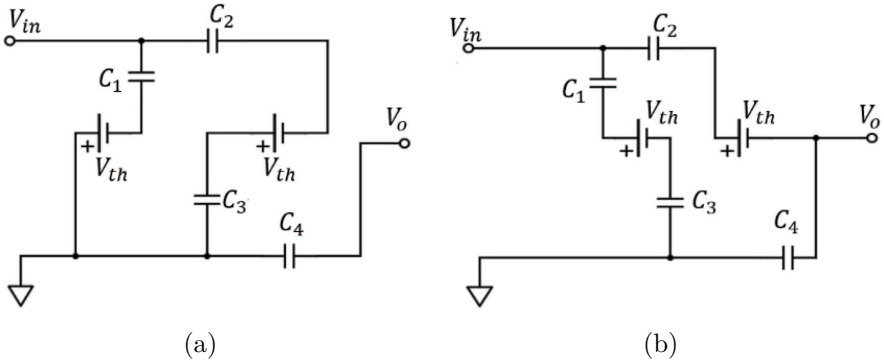

FIGURE 2. Instantaneous equivalent circuits of the Dickson converter: (a) State 1 and (b) state 2

the instantaneous equivalent circuit when the input voltage V_{in} is positive. During state 2, the diodes D_2 and D_4 are driven by the positive input voltage. As a result, the capacitors C_3 and C_4 are charged.

The voltage charged to each capacitor is expressed as

$$V_{C_1} = V_{in} - V_{th} \tag{3}$$
$$V_{C_3} = V_{in} + V_{C_1} - V_{th} = 2(V_{in} - V_{th}) \tag{4}$$
$$V_{C_2} = V_{in} + V_{C_3} - V_{th} = 3(V_{in} - V_{th}) \tag{5}$$
$$V_{C_4} = V_{in} + V_{C_2} - V_{th} = 4(V_{in} - V_{th}) \tag{6}$$

In Equation (3), V_{in} is the input voltage, V_{th} denotes the diode threshold voltage, V_{C_1}, to V_{C_4} indicate the voltage of each capacitor. Since a single Dickson converter realizes a DC voltage with the four times gain, the voltage gain of the conventional circuit is eight times.

Figures 3, 4 and 5 illustrate the circuit configuration of the proposed converters. The proposed converters are designed by employing the conventional circuit shown in Figure 1 and the traditional switching converter with a single inductor, where the proposed circuit shown in Figure 3 provides a stepped-up voltage by using a boost converter, the proposed circuit shown in Figure 4 generates a stepped-down voltage by using a buck converter, and the proposed circuit shown in Figure 5 offers a stepped-up or stepped-down voltage by using a buck-boost converter. Unlike the conventional converter shown in Figure 1, the proposed converters can achieve output voltage controllability. Therefore, the proposed circuits can adjust the output voltage by controlling the duty cycle D although the vibration input is unstable.

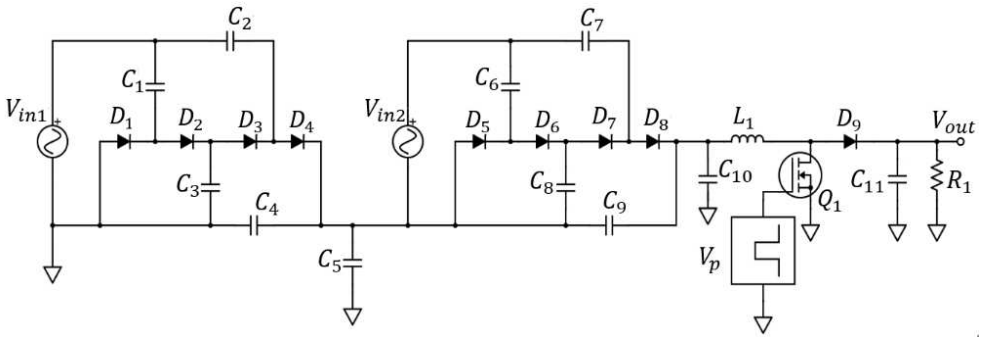

FIGURE 3. Proposed circuit with boost converter

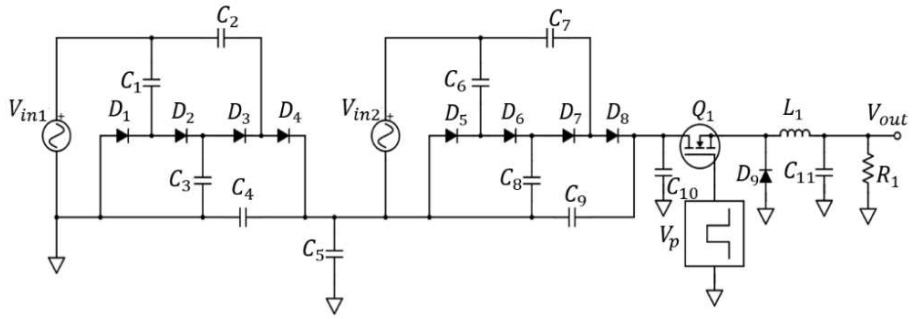

FIGURE 4. Proposed circuit with buck converter

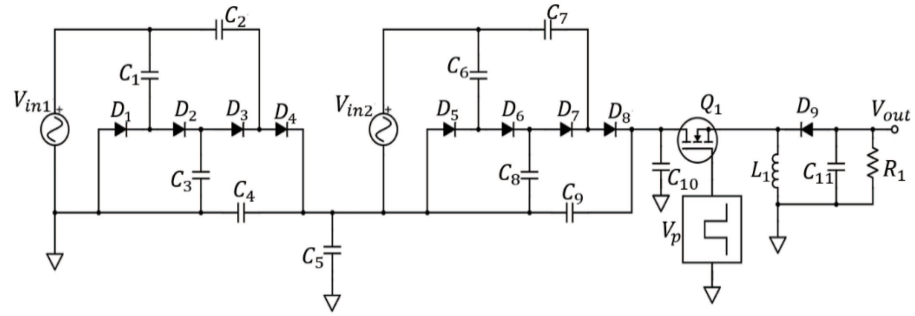

FIGURE 5. Proposed circuit with buck-boost converter

The operation principle of Figure 3 is as follows. While the switch Q_1 is on, energy is charged to the inductor L_1 by the output voltage V_o of the front stage. On the other hand, while Q_1 is off, the output energy of the front stage is combined with the energy stored in L_1 and is provided as the output voltage V_{out}. In continuous conduction mode (CCM), the output voltage is expressed as

$$V_{out} = \frac{1}{1-D} V_o \tag{7}$$

The operation principle of Figure 4 is as follows. While the switch Q_1 is on, energy is charged to the inductor L_1 by the output voltage V_o of the front stage. On the other hand, while Q_1 is off, the energy stored in L_1 is provided as the output voltage V_{out}. In continuous conduction mode (CCM), the output voltage is expressed as

$$V_{out} = DV_o \tag{8}$$

The operation principle of Figure 5 is as follows. While the switch Q_1 is on, energy is charged to the inductor L_1 by the output voltage V_o of the front stage. On the other hand, while Q_1 is off, the energy stored in L_1 is provided as the output voltage V_{out}. In continuous conduction mode (CCM), the output voltage is expressed as

$$V_{out} = -\frac{D}{1-D} V_o \tag{9}$$

The Dickson converter in the front stage performs AC/DC conversion and boosts the voltage at the same time. Then, the output voltage of the front stage is converted into various voltages by the three types of converters.

3. **SPICE Simulation.** SPICE simulations were performed to clarify the effectiveness of the proposed circuit. In this simulation, the proposed circuits are compared with the conventional circuit.

3.1. **Simulation conditions.** The input is assumed as V_{in} = 3 V @ 50Hz from the AC constant voltage power supply. The capacitor is an ideal capacitor with the capacitance 3.3 mF. The transistor switch is modelled by the ideal switch with the on-resistance 1 Ω. The operating frequency f is 1 MHz. The duty ratio was varied from 0.3 to 0.7 and the output load was set to 100 Ω, 300 Ω, 500 Ω, 700 Ω, 1 kΩ, 2 kΩ, 3 kΩ, 4 kΩ, 5 kΩ, 6 kΩ, and 7 kΩ.

3.2. **Simulation result.** First, the simulated voltage gain of the conventional circuit is shown in Figure 6(a). As this figure shows, the conventional circuit can provide the voltage gain of about 9 times. Next, the simulated voltage gain of the proposed circuit using the boost converter is depicted in Figure 6(b). In this figure, the voltage gain is 11 to 26 times. Then, the simulated voltage gain of the proposed circuit using the buck converter is illustrated in Figure 6(c). As it can be seen from this figure, the voltage gain is about 2.4 to 6.6 times. Finally, the simulated voltage gain of the proposed circuit using the buck-boost converter is presented in Figure 6(d). In this figure, the voltage gain is about −3.1 to −19.6 times.

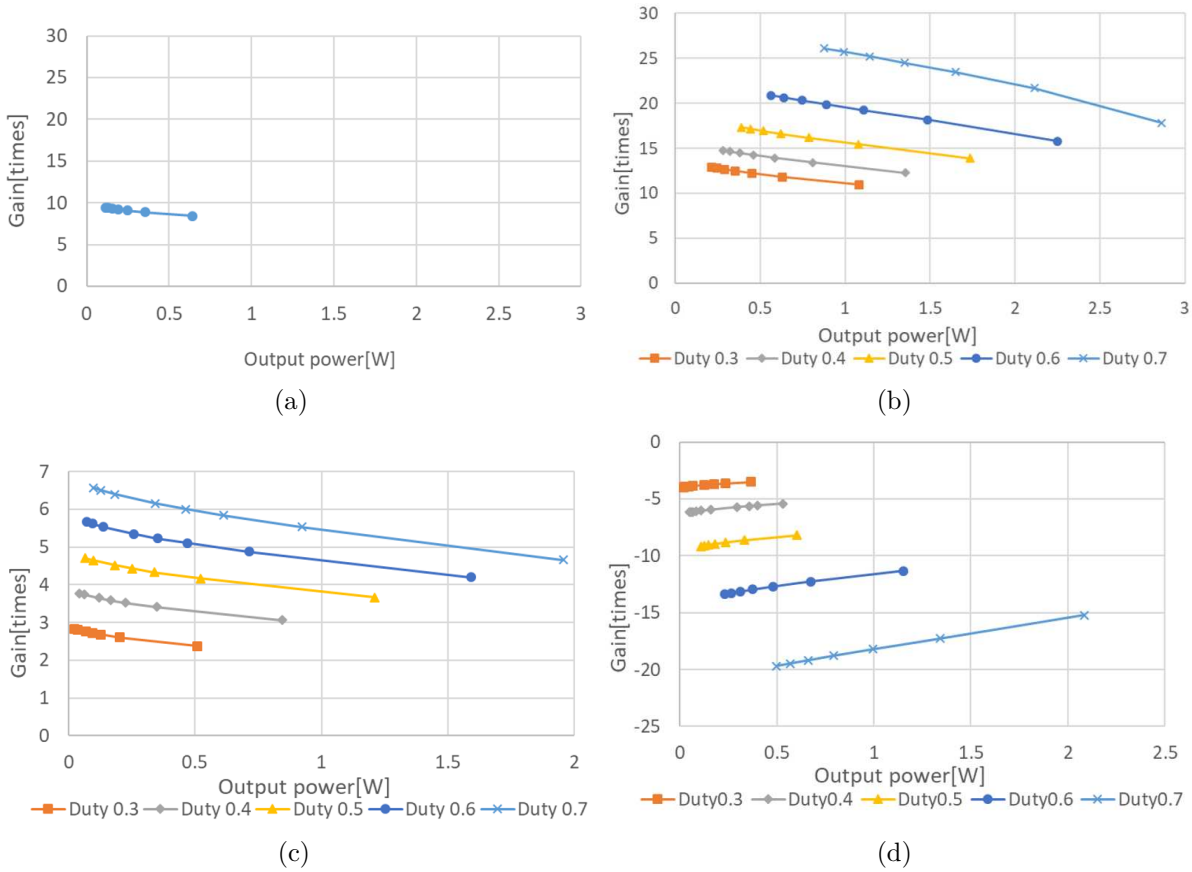

FIGURE 6. Output power and gain of simulation results: (a) Conventional converter, (b) boost converter, (c) buck converter, and (d) buck-boost converter

The simulated power efficiency of the conventional circuit is shown in Figure 7(a). As this figure shows, the conventional circuit can provide the maximum power efficiency of about 84%. Next, the simulated power efficiency of the proposed circuit using the boost converter is depicted in Figure 7(b). In this figure, the maximum power efficiency is about 77%. Then, the simulated power efficiency of the proposed circuit using the buck converter is illustrated in Figure 7(c). As it can be seen from this figure, the maximum power efficiency is about 80%. Finally, the simulated power efficiency of the proposed

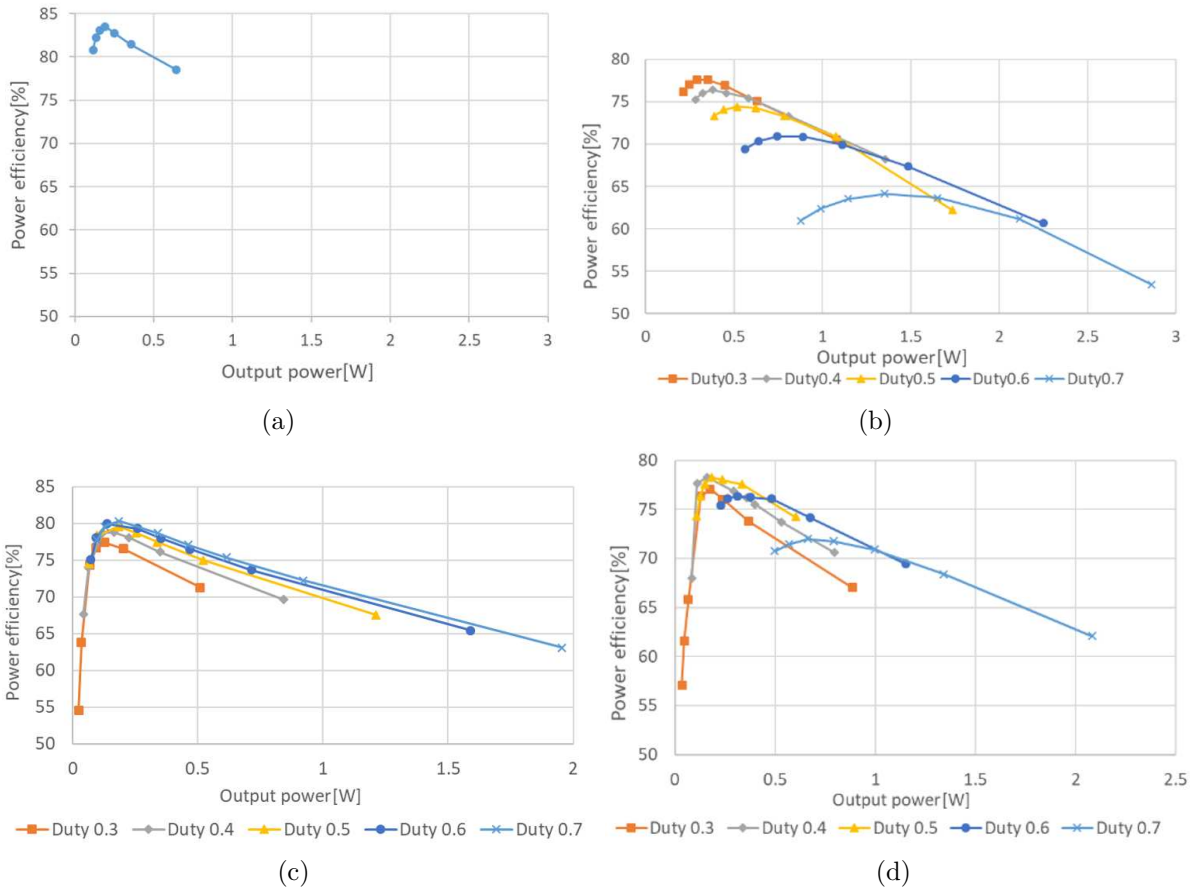

FIGURE 7. Output power and power efficiency of simulation results: (a) Conventional converter, (b) boost converter, (c) buck converter, and (d) buck-boost converter

circuit using the buck-boost converter is presented in Figure 7(d). In this figure, the maximum power efficiency is about 78%.

4. **Experiment.**

4.1. **Experimental conditions.** The experimental circuit was built on the PCB to confirm the feasibility of the proposed topologies. The circuit components to assemble the experimental circuit are shown in Table 1, where the n-type MOSFET is 2SK447, the Schottky barrier diode is 11EQS03L, and the capacitor is an electrolytic capacitor 3.3 mF. The instruments used in the experiment are shown in Table 2. In the experiment, the power supply for the experimental circuit is a low frequency oscillator AG203D manufactured by KENWOOD. The function generator was used as the driver circuit for operating the switch. The KEYSIGHT oscilloscope MSOX2014A is used to measure the input/output voltage. The square wave generated by the function generator was set to 50 kHz in the proposed circuit using the boost converter. In addition, the buck converter and buck boost converter were set to 500 kHz. Experiments were conducted using the output load resistor of 100 kΩ, 150 kΩ, 200 kΩ, 330 kΩ, and 510 kΩ for the boost converter and 200 Ω, 330 Ω, 500 Ω, 750 Ω, 1 kΩ, and 2 kΩ for the buck and buck-boost converters. The experiments are conducted under the conditions that the input power supply of 1.5 V @ 50 Hz for the boost converter and the input power supply of 2.3 V @ 50 Hz for the buck and buck-boost converters.

4.2. **Experimental result.** The results of the experiment are shown in Figure 8. In this figure, the voltage gains of the boost converter, buck converter, and buck-boost converter

TABLE 1. Circuit components used in the experiment

Part name	Manufacturer
Universal substrate	Picotec International Co., Ltd.
Schottky barrier diode (11EQS03L)	Nihon Inter Electronics Corporation
MOSFET (2SK447)	Toshiba
Isolation transformer	TOYOZUMI
Micro inductor 10 mH	Core Master Enterprise
Electrolytic capacitor 3.3 mF	Rubycon
Carbon resistance	FAITHFUL LINK INDUSTRIAL

TABLE 2. Instruments used in the experiment

Equipment name	Model number	Manufacturer
Low frequency oscillator circuit	AG203D	TEXIO
Function generator	SG4262	IWATSU
Oscilloscope	MSOX2014A	KEYSIGHT

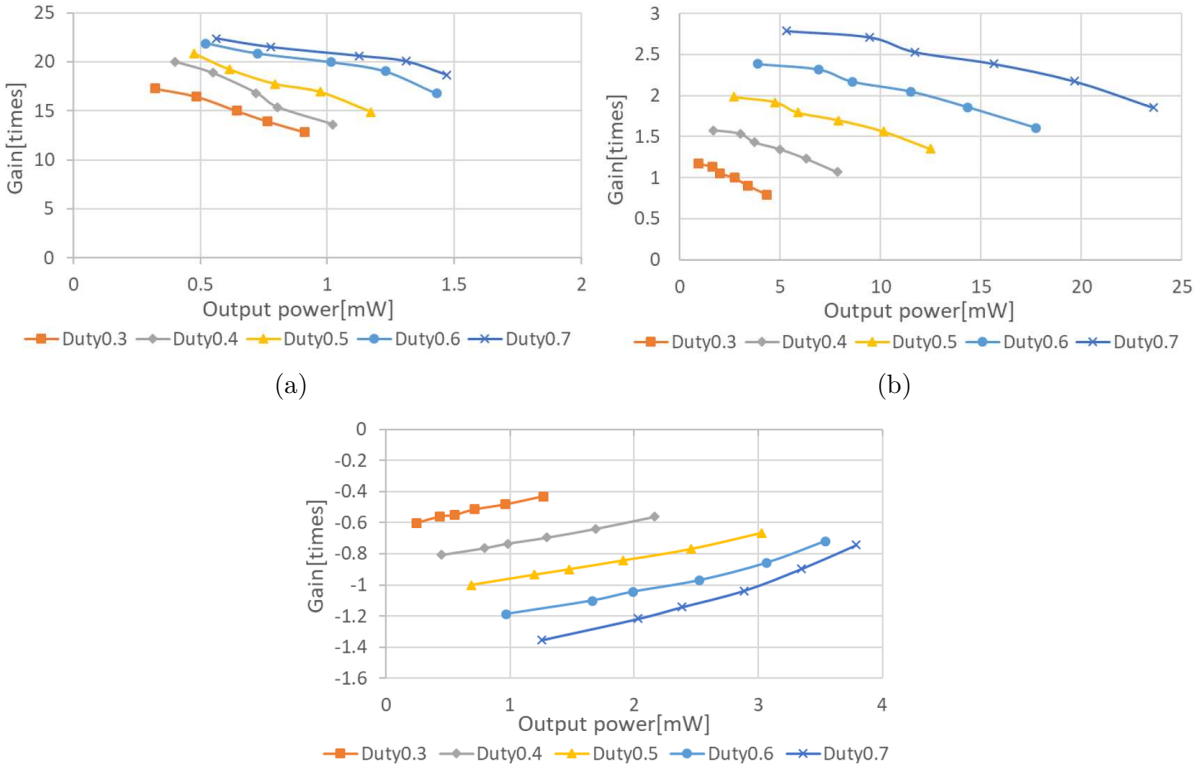

FIGURE 8. Output power and gain of experimental results: (a) Boost converter, (b) buck converter, and (c) buck-boost converter

are 12.8 to 22.4 times, 0.8 to 2.8 times, and −0.43 to −1.35 times, respectively. The maximum output power of the boost converter, buck converter, and buck-boost converter is 1.47 mW, 24 mW, and 3.8 mW, respectively. All of the proposed circuits can change gain by controlling the duty ratio.

5. **Conclusions.** For vibration energy harvesting, we proposed three types of MISO AC/DC converters with a single inductor. Unlike the conventional circuit, the proposed circuits can achieve various gains by changing the duty ratio. The SPICE simulations

showed that only about 9 times the output gain could be obtained with the conventional circuit. In contrast, the proposed circuit achieved a wider range of output gain than the conventional circuit by varying the duty ratio of switching from 0.3∼0.7. A future challenge is to improve the power efficiency by introducing soft-switching techniques into the proposed circuit.

REFERENCES

[1] Y. Kuang and M. Zhu, Characterisation of a knee-joint energy harvester powering a wireless communication sensing node, *Smart Mater. Struct.*, vol.25, no.5, 055013, 2016.

[2] T. Ruan, Z. J. Chew and M. Zhu, Energy-aware approaches for energy harvesting powered wireless sensor nodes, *IEEE Sensors Journal*, vol.17, no.7, pp.2165-2173, DOI: 10.1109/JSEN.2017.2665680, 2017.

[3] D. Guyomar and M. Lallart, Recent progress in piezoelectric conversion and energy harvesting using nonlinear electronic interfaces and issues in small scale implementation, *Micromachines*, vol.2, no.2, pp.274-294, 2011.

[4] M. A. Mohammed, F. F. Mustafa and F. I. Mustafa, Feasibility study for using harvesting kinetic energy footstep in interior space, *2020 11th International Renewable Energy Congress (IREC)*, pp.1-4, DOI: 10.1109/IREC48820.2020.9310416, 2020.

[5] T. C. Huang et al., 120% harvesting energy improvement by maximum power extracting control for high sustainability magnetic power monitoring and harvesting system, *IEEE Trans. Power Electronics*, vol.30, no.4, pp.2262-2274, 2015.

[6] E. J. Carlson, K. Strunz and B. P. Otis, A 20 mV input boost converter with efficient digital control for thermoelectric energy harvesting, *IEEE Journal of Solid-State Circuits*, vol.45, no.4, pp.741-750, DOI: 10.1109/JSSC.2010.2042251, 2010.

[7] C. Alippi and C. Galperti, An adaptive system for optimal solar energy harvesting in wireless sensor network nodes, *IEEE Trans. Circuits and Systems I: Regular Papers*, vol.55, no.6, pp.1742-1750, 2008.

[8] G. Shi, Y. Xia, H. Xia, X. Wang, L. Qian, Z. Chen, Y. Ye and Q. Li, An efficient power management circuit based on quasi maximum power point tracking with bidirectional intermittent adjustment for vibration energy harvesting, *IEEE Trans. Power Electronics*, vol.34, no.10, pp.9671-9685, DOI: 10.1109/TPEL.2019.2892457, 2019.

[9] A. Shareef, W. L. Goh, S. Narasimalu and Y.Gao, A rectifier-less AC/DC interface circuit for ambient energy harvesting from low-voltage piezoelectric transducer array, *IEEE Trans. Power Electronics*, vol.34, no.2, pp.1446-1457, DOI: 10.1109/TPEL.2018.2831714, 2019.

[10] K. Abe, K. Smerqitak, S. Pongswatd, I. Oota and K. Eguchi, A step-down switched-capacitor AC/DC converter with double conversion topology, *International Journal of Innovative Computing, Information and Control*, vol.13, no.1, pp.319-330, DOI: 10.24507/ijicic.13.01.319, 2017.

[11] K. Eguchi and A. Shibata, An inductor-less step-up multi-input single-output AC/DC converter for vibration energy harvesting, *IEEJ Trans. Electrical and Electronic Engineering*, vol.16, pp.170-172, DOI: 10.1002/tee.23281, 2021.

[12] W. Do and K. Eguchi, A new type of switched capacitor converter for energy harvesting system, *Energy Reports*, vol.8, no.1, pp.942-948, DOI: 10.1016/j.egyr.2021.11.105, 2022.

[13] W. Do, H. Bevrani, Q. Shafiee and K. Eguchi, An analytical approach for design of a cross-connected Fibonacci switched capacitor converter, *Energies*, vol.13, no.2, DOI: 10.3390/en13020431, 2020.

[14] K. Eguchi, S. Hirata, M. Shimoji and H. Zhu, Design of a step-up/step-down k $(= 2, 3, \ldots)$-Fibonacci DC-DC converter designed by switched-capacitor techniques, *2012 5th International Conference on Intelligent Networks and Intelligent Systems*, pp.170-173, DOI: 10.1109/ICINIS.2012.67, 2012.

[15] K. Eguchi, D. Nakashima, T. Ishibashi and I. Oota, A multi-input single-output Dickson-type AC/DC converter for vibration energy harvesting, *Energy Reports*, vol.7, no.6, pp.78-83, DOI: 10.1016/j.egyr.2021.08.070, 2021.